A cost model with several hydraulic constraints for optimizing in practice a trapezoidal cross section

Kiyoumars Roushangar, Mohammad Taghi Alami, Vahid Nourani and Aida Nouri

ABSTRACT

Open channel structures are essential to infrastructure networks and expensive to manufacture. Optimizing the design of channel structures can reduce the total cost of a channel's length, including costs of lining, earthwork, and water lost through seepage and evaporation. The present research aims to present various optimization models towards the design of trapezoidal channel cross section. First, a general resistance equation was applied as a constraint. Next, a genetic algorithm (GA) was used to determine the optimal geometry of a trapezoidal channel section based on several parameters, i.e., depth, bottom width, and side slope. Eight different models were proposed and evaluated with no other constraint besides financial cost as well as with a normal depth, flow velocity, Froude number, top width, and by ignoring the cost of seepage. Numerical outcomes obtained by the GA are compared to previous studies in order to determine the most efficient model. Results from a single application indicate that the restriction of depth, velocity, and Froude number can increase the total cost, while restriction of the top width can decrease the cost of the construction. Also, the solution for various example problems incorporating different discharge values and bed slopes caused increase and decrease in cost, respectively.

Key words | hydraulic parameters, open channels, optimization, trapezoidal section

Kiyoumars Roushangar (corresponding author)
Mohammad Taghi Alami
Vahid Nourani
Aida Nouri
Department of Civil Engineering,
University of Tabriz,
Tabriz,
Iran
E-mail: *kroshangar@yahoo.com*

Vahid Nourani
Department of Civil Engineering,
Near East University,
Nicosia,
North Cyprus, Mersin 10,
Turkey

NOTATION

A	flow area of channel (m^2)
b	bed width of channel (m)
C	cost per unit length of canal ($/m)
C_e	cost of earthwork per unit length of channel ($/m)
C_L	cost of lining per unit length of channel ($/m)
C_w	capitalized cost of water lost per unit length of channel ($/m)
c_e	cost per unit volume of earthwork at ground level ($/$m^3$)
c_L	cost per unit surface area of lining ($/$m^2$)
c_r	increase in unit excavation cost per unit depth ($/$m^4$)
c_w	cost per unit volume of water ($/$m^3$)
E	evaporation discharge per unit free surface area (m/s)
Fr	Froude number
Fs	seepage function (dimensionless)
g	gravitational acceleration (m/s^2)
k	hydraulic conductivity (m/s)
m	side slope of channel (dimensionless)
P	flow perimeter of channel (m)
p	penalty parameter (dimensionless)
Q	discharge (m^3/s)
R	hydraulic radius (m)
S_0	bed slope of channel (dimensionless)
T_w	top width (m)
V	average velocity (m/s)
y_n	normal depth of flow in channel (m)
ε	average roughness height of canal lining (m)
λ	length scale (m)

doi: 10.2166/hydro.2017.081

ν kinematic viscosity (m^2/s)
ϕ equality constraint (dimensionless)
Ψ augmented function (dimensionless)
$ monetary unit

INTRODUCTION

Irrigation channel networks are very substantial and are utilized as water supply and conveyance facilities, flood control and for use in other fields. Due to the high cost of channel construction, investigating the optimal and economic cross-sectional designs of these channels is a necessity. A channel in the network may be subjected to lining. The supported cost of a lined channel is less in comparison to unlined channels, since the lining protects against bed and bank erosion. Channels in alluvium are typically lined and capable of decreasing seepage. The seepage loss from channels has been estimated for different sets of special conditions. The analytical form of these solutions, which contain complex integrals and unknown implicit state variables, is not convenient in designing or estimating seepage from the existent channels (Morel-Seytoux 1964; Garg & Chawla 1970; Subramanya *et al.* 1973; Sharma & Chawla 1979).

Swamee *et al.* (2000) considered seepage loss in the objective functions and applied nonlinear optimization techniques to design explicit equations. Wachyan & Rushton (1987) used empirical measurements to reveal that main losses occurring from channels are related to whether they are lined or unlined. Kacimov (1992) developed a complex-variable method to optimize the shape design problems of channel beds. In order to minimize the cost function, the seepage losses and cost of lining was constrained by specified hydraulic characteristics. Additionally, Aksoy & Altan-Sakarya (2006) studied the optimum values of section variables for different channel types by minimizing their cost.

Usually, evaporation from a channel is only a small proportion of the total loss, but it becomes substantial for long channels running through arid regions. Warnaka & Pochop (1988) and Ikebuchi *et al.* (1988) compared the capabilities of different evaporative sorts of estimation models and found that the mass transfer-based models presented the most accurate results (Fulford & Sturm 1984).

The primary factor affecting the channel design is the channel surface forming material which determines the roughness coefficient, the minimum permissible velocity to avoid deposition of silt or debris, the constrained velocity to prevent erosion of the channel surface, and the topography of the channel route which indicates how much the section is hydraulically and/or economically efficient (Chow 1973). The choice of hydraulic parameters is a vital task in the hydraulic design of channels since they are entitled to high uncertainty. Dimitriadis *et al.* (2016) employed extended sensitivity analysis by simultaneously varying the input discharge, longitudinal and lateral gradients and roughness coefficient.

Monadjemi (1994) and Froehlich (1994) modeled optimized channel design using a Lagrangian undetermined multiplier method. Alternatively, for non-linear, non-convex optimization problems, the compound and implicit construction of the cost function and/or constraints makes the employment of customary gradient-based techniques very difficult, so that the optimization process cannot be applied in many locally optimized processes. This has caused the wide use of heuristic approaches, e.g., genetic algorithm (GA) (Goldberg 1989), particle swarm optimization (PSO) (Kennedy & Eberhart 1995), genetic programming (GP) (Koza 1992), gene expression programming (GEP) (Azamathulla 2012), and charged system search (Kaveh & Talatahari 2010), among many others. Different optimization algorithms are applied to open channel section design problems.

The GA has been successfully utilized for optimizing the design of open channels (Jain *et al.* 2004; Bhattacharjya & Satish 2007), as well as irrigation scheduling with flow of water through channel networks (Nixon *et al.* 2000), along with other hydraulic problems (Wu & Simpson 2002; Roushangar & Koosheh 2015). The GP has been applied in different engineering optimization problems (Sharifi *et al.* 2011). The GEP approach has also been used to solve engineering problems by deriving a new predictive model (Azamathulla & Ahmad 2013; Azamathulla 2013). PSO also has been successfully applied for solving water resources management problems (Janga Reddy & Nagesh Kumar 2009). Also Nourani *et al.* (2009) optimized composite channels using ant colony optimization.

To the authors' knowledge, despite considerable investigations into providing a protocol for minimizing cross-sectional area of channels, there are no investigations

dealing with constrained hydraulic parameters as well as the role of seepage cost on optimal channel sections. Therefore, in this study, six different models of optimum design for open channels were established. The first model was evaluated with no additional constraint equation, while in the second model, the channel top width was considered as an additional constraint. The third and fourth models had additional constraints of different values of velocity and Froude numbers, respectively. The fifth model utilized additional constraint of different depth values. The sixth model was determined for no seepage cost state. Finally, the applications section shows the effect of discharge (seventh model) and longitudinal bed slopes (eighth model) on optimum design of channels. We applied all models to a real case scenario and showed that the constrained hydraulic parameters have a great influence in the design of the trapezoidal channel section.

FORMULATION OF OPTIMAL DESIGN OF OPEN CHANNELS

Selection of the geometric variables, e.g., side slope, bottom width, and flow depth for open channel sections varies according to the designer's perspective. Also, the longitudinal bed slope of the channel is influenced by topography that is considered as a constant amount in seven models. One of the important objectives is minimizing the total cost of a channel section, that it has the capability of passing the channel distance safely, which must be considered. Generally, the cost per unit length of a lined open channel section is defined as the summation of three terms, namely, the depth-dependent earthwork cost, the cost of lining, and the cost of water lost as seepage and evaporation. These terms are explained in the following sections.

Earthwork cost, lining cost, and cost of water loss

The total cost function of the channel per unit length C (\$/m) was obtained as:

$$C = C_e + C_l + C_w = c_e A + c_r A\bar{y} + c_l P + c_{ws} F_s y_n + c_{we} T_w \quad (1)$$

The earthwork cost C_e (monetary unit per unit length, e.g., \$/m) is given as:

$$C_e = c_e A + c_r A\bar{y} \quad (2)$$

where c_e = cost per unit volume of earthwork at ground level (\$/m^3); c_r = the additional cost per unit volume of excavation per unit depth (\$/m^4); A = flow area (m^2); $\bar{y}$ = depth of the centroid of the area of excavation from the ground surface (m).

The cost of lining C_l (monetary unit per unit length, e.g., \$.m^{-1}) is expressed as:

$$C_l = c_l P \quad (3)$$

where c_l = cost of unit lining (monetary unit per unit area of lining, e.g., \$.m^{-2}) and P = flow perimeter (m). The capitalized cost of water lost C_w (\$/m) might be expressed as:

$$C_w = c_{ws} y_n F + c_{wE} T_w \quad (4)$$

$$c_{ws} = 3.156 \times 10^7 k^{c_w}/r \quad (5)$$

$$c_{wE} = 3.156 \times 10^7 E^{c_w}/r \quad (6)$$

where r = rate of interest (\$/\$/year) and c_w = cost per unit volume of water (\$/m^3). The volumetric cost of water may differ for evaporation and seepage losses, depending upon the side effects caused by the seepage loss. k = coefficient of permeability (m/s); y_n = normal depth of flow in the channel (m); and Fs = seepage function (dimensionless), which depends on channel geometry. T_w = width of free surface (m); and E = evaporation discharge per unit surface area (m/s) (Swamee *et al.* 2000). The c_l/c_e and c_e/c_r ratios were obtained as listed in Table 1 (Schedule of rates 1997). These ratios can be obtained for various kinds of linings, soil strata, and climatic conditions by utilizing appropriate unit rates.

The objective function of this research is taken to be the reduction of cost. The uniform flow equation is treated as a restriction and is inserted into the optimization models. A rigid boundary irrigation channel is designed by exploiting the uniform flow resistance equation. The most commonly used uniform flow resistance formula is the Manning equation

Table 1 | The following are dimensionless equations

Dimensionless variables

$\varepsilon_* = \varepsilon/\lambda$	$\nu_* = \nu\lambda/Q$	$C_* = C/(c_e\lambda^2)$	$C_{l*} = C_l/(C_e\lambda)$	$C_{r*} = C_r\lambda/C_e$	$C_{ws*} = C_{ws}/c_e\lambda$	$C_{wE*} = C_{wE}/c_e\lambda$
$\bar{y}_* = \frac{\bar{y}}{\lambda}$	$P_* = P/\lambda$	$T_{w*} = T/\lambda$	$A_* = A/\lambda^2$	$R_* = R/\lambda$	$y_{n*} = y_n/\lambda$	

(Chow 1973), which is suitable for rough turbulent flow and in a limited band-width of relative roughness (Christensen 1984). Relaxing these restrictions, Swamee (1994) gave a more general resistance equation based on roughness height:

$$V = -2.457\sqrt{gRS_0}\ln\left(\frac{\varepsilon}{12R} + \frac{0.221\vartheta}{R\sqrt{gRS_0}}\right) \tag{7}$$

where V = average flow velocity (m/s); g = gravitational acceleration (m/s^2); R = hydraulic radius (m); S_0 = longitudinal bed slope (dimensionless); ε = average roughness height of the channel lining (m); and ϑ = kinematic viscosity of water (m^2/s). Utilizing the continuity equation, the discharge Q (m^3/s) was obtained as:

$$Q = AV = -2.457A\sqrt{gRS_0}\ln\left(\frac{\varepsilon}{12R} + \frac{0.221\vartheta}{R\sqrt{gRS_0}}\right) \tag{8}$$

Combining Equations (1) and (8) forms the general optimization algorithm for a minimum cost section of open channel. The terms of these models are all in dimensional forms. In order to facilitate the detection of the effects of variables on the models, the aforementioned equations are transformed to dimensionless forms, through defining a length scale, as follows:

$$\lambda = (Q/\sqrt{gS_0})^{0.4} \tag{9}$$

The following dimensionless variables were then obtained in Table 1. The subscript * denotes the corresponding dimensionless parameters of each hydraulic parameter.

Using Equations (1) and (8), and Table 1, the problem of determining the optimal channel section formed in dimensionless form is reduced to:

$$Minimize\ C_* = A_* + C_{r*}A_*\bar{y} + C_{l*}P_* + C_{ws*}F_s y_n + C_{wE*}T_w \tag{10}$$

$$\text{Subject to } \phi_1 = 1 + 2.457\mathrm{A}_*\sqrt{\mathrm{R}_*}\ln\left(\frac{\varepsilon_*}{12\mathrm{R}_*} + \frac{0.221\vartheta_*}{\mathrm{R}_*^{1.5}}\right) \tag{11}$$

where ϕ = equality restriction function.

The restriction optimization problem (i.e., Equations (10) and (11)) was solved by minimizing the augmented function ψ distributed by:

$$\Psi = C_* + \alpha\sum_{i=1}^{I}\phi^{\beta} \tag{12}$$

where β = exponent of equality constraint function ($0 < \beta \leq 2$); α = penalty function parameter with a high positive value; i = index representing restriction; and I = total number of restrictions imposed on a particular nonlinear optimization programming (NLOP). The optimum design was applied on trapezoidal channel cross sections (Figure 1). According to Figure 1, the bottom width, flow depth, and side slope are represented by b (m), y_n (m), and m, respectively. Consequently, the equations are as follows:

$$A_* = (b_* + my_{n*})y_{n*} \tag{13}$$

$$P_* = b_* + 2y_{n*}\sqrt{1+m^2} \tag{14}$$

$$T_{w*} = b_* + 2my_{n*} \tag{15}$$

$$Fr = \frac{V}{\sqrt{gD}} \tag{16}$$

$$D = \frac{A}{T_w} \tag{17}$$

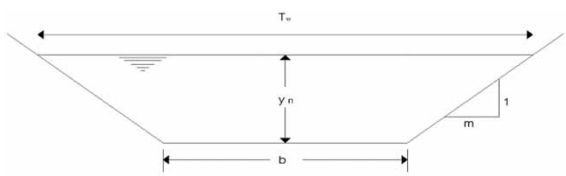

Figure 1 | A trapezoidal channel cross section.

PROCEDURES FOR OPTIMAL DESIGN

Validation with using empirical equations

Analysis of the optimal channel sections for a number of input variables led to the following generalized empirical equations in clear form for trapezoidal channel section (Swamee *et al.* 2000).

For a given set of data, a channel can be designed by minimizing Equation (10) and subjected to constraint given by Equation (11). Swamee's method is used to verify the results.

GA-based optimization procedure

The GA is employed to solve the formulated nonlinear models. The GA is a search technique based on the genetics concept of natural selection, which combines an artificial survival of the fittest with genetic operators abstracted from nature (Holland 1975). The important difference between GA and classical optimization search techniques is that the GA generates a population of possible solutions, whereas the classical optimization techniques lead to a single solution. An individual solution in a population of solutions is analogous to a biological chromosome. While a natural chromosome specifies genetic characteristics of a human being, an artificial chromosome in GA indicates the values of varied decision variables representing a decision or a solution. For most GAs, candidate solutions are represented by chromosomes coded using a binary number system (Goldberg 1989). The GA that employs binary strings as its chromosomes is named binary-coded GA. The binary-coded GA contains three basic operators: selection, crossover or mating, and mutation. The selection function chooses parents for the next generation based on their scaled values from the fittest scaling function. In this study, the stochastic uniform selection is used in conjunction with elitism. The stochastic uniform selection lays out a line in which each parent corresponds to a section of the line of length proportional to its expectation.

Crossover combines two individuals or parents to form a new individual or child for the next generation. The scattered crossover operator is employed in this study. Scatter creates a random binary vector. Mutation functions make small random changes in the individuals in the population which provide genetic diversity and enable the GA to search a broader space. In the present study, constraint-dependent default is used. Three main steps of GA generate the solutions (Goldberg 1989). Figure 2 shows these following steps: (1) select the individuals as parents considering the best objective value; (2) crossover the parents to form the next generation; (3) add random changes to the population (mutation). This method consists of eight models (Figure 3).

Model I

This model is determined by Equations (10) and (11), representing no additional constraint when consisting of three variables.

Model II

There are several cases where the top width must be constrained. Then, an additional restriction could be imposed on the NLOP represented by Equations (10) and (11). The optimization formulation remains the same, except the following additional restriction is imposed to restrict the top width to T_{wmax}:

$$\phi_2 = T_{wmax-}T_{wt} \geq 0 \tag{18}$$

where $\phi_2 =$ additional equality constraint function which limits the total top width of the channel to T_{wmax}.

Model III

If the average velocity of the channel is more comparable to the permissible velocity of the channel, the average velocity can be constrained utilizing the following restriction:

$$\phi_3 = a - v_{av} \geq 0 \tag{19}$$

where $a =$ maximum velocity and $v_{av} =$ average velocity of the channel.

For the designed section, the average flow velocity V_{av} could be achieved by Equation (8). However, in order to safely convey the required discharge through a channel, it is necessary to ensure that the velocity of the channel does

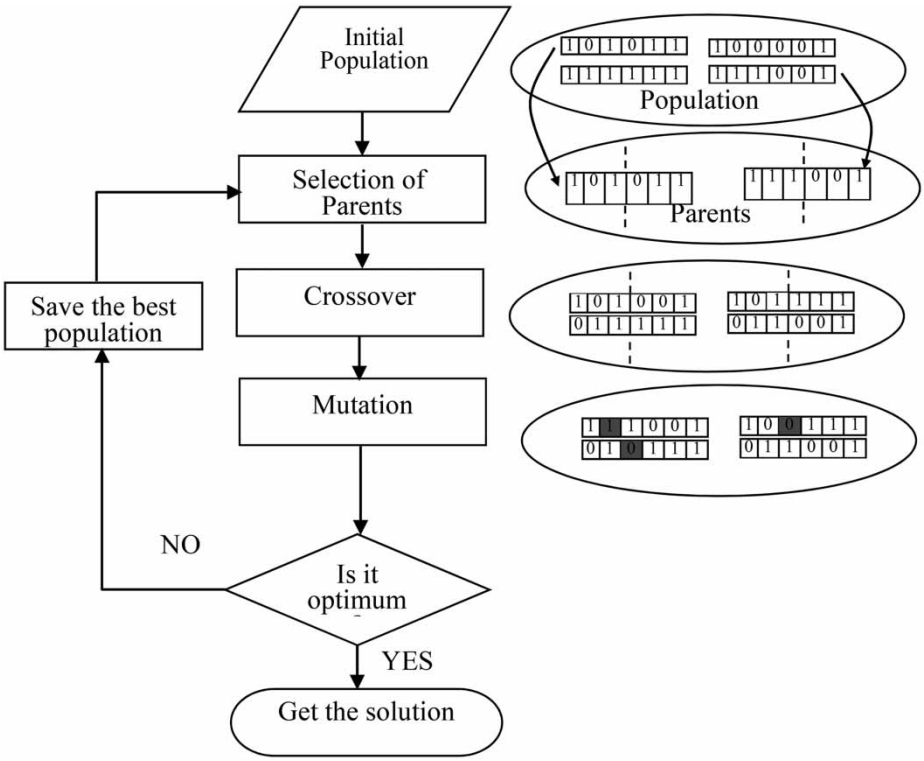

Figure 2 | Flowchart of genetic algorithm.

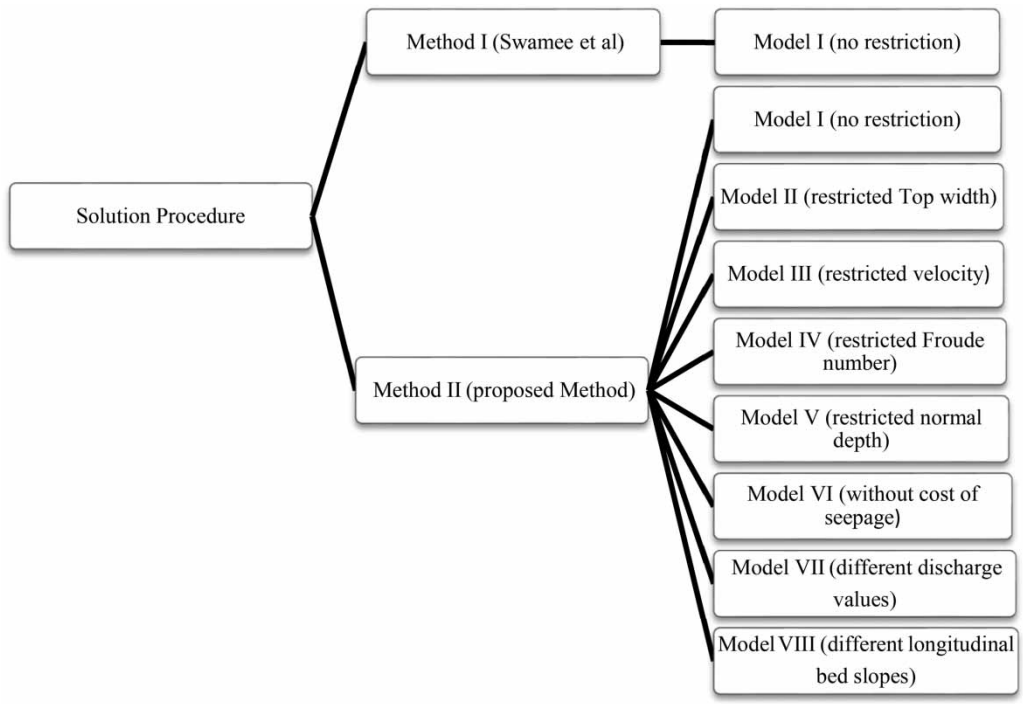

Figure 3 | Solution procedures.

not exceed the corresponding maximum velocity which is related to the roughness coefficient of that segment.

Model IV

There are several cases where the flow of channel constrains the Froude number of the channel:

$$\phi_4 = F_{rmax} - F_r \geq 0 \quad (20)$$

where F_{max} = maximum permissible Froude number.

Model V

In the case of the existence of unfavorable strata, depth of channel should not exceed a certain limit. This may require a restriction on the maximum permissible flow depth. Thus, the limiting depth model could be addressed in the channel design problem by imposing Equation (21) as an additional constraint to the optimization formulation involving Equations (10) and (11):

$$\phi_5 = y_{max} - y_n \geq 0 \quad (21)$$

Model VI

The objective function has been investigated without cost of seepage to observe the influence of seepage on hydraulic parameters of a channel with constraint (Equation (11)):

$$\text{Minimize } C_* = A_* + C_{r*}A_*\bar{y} + C_{l*}P_* + C_{ws*}F_s y_n + C_{wE*}T$$

RESULTS AND DISCUSSION

Let us suppose that the channel should be designed to transport a discharge of 100 m^3/s on a longitudinal bed slope of 0.001. The channel passes through a stratum of typical soil, in which $\frac{C_e}{C_r} = 7$ m and $\frac{C_{ws}}{C_e} = 10$ m (Table 2). Further, it is proposed to supply concrete lining with $\frac{C_l}{C_e} = 12$ m. The climatic condition of the channel area satisfies the $\frac{C_{wE}}{C_e} = 2$ m. For the purpose of design, it is assumed that $g = 9.79$ (m/s^2), $\vartheta = 1.1 \times 10^{-6} (m^2/s)$ (water at 20 °C), and $\varepsilon = 1$ mm (concrete lining) (Table 3).

Using Equation (9), the λ was determined to be 15.9 m, so the following parameters were identified using Equation (10): $\varepsilon_* = 6.3 \times 10^{-5}$, $\vartheta_* = 1.75 \times 10^{-7}$, $C_{l*} = 0.75$, $C_{r*} = 2.27$, $C_{ws*} = 0.63$, and $C_{wE*} = 0.125$.

Table 4 compares the Swamee method (Swamee *et al.* 2000) with the proposed GA-based Model I of the present study (no additional constraint model). The sum total construction costs in both methods for Model I (no additional restriction) are 429.27 and 417.26, respectively. It can be noted from Table 4 that the proposed GA-based model shows better results compared to the Swamee method, with relatively less expensive values.

Table 5 represents the optimization results for different values of channel top width as an additional constraint (Model II). The table clearly shows that decreasing the channel top width leads to lower costs. Figure 4 displays the channel top width (T_{w*}) effect on dimensionless area (A_*) and total cost (C_*) values. From Figure 4 it is clear that the

Table 2 | Lining and earthwork cost coefficients (Schedule of rates 1997)

	cl/ce (m)									
	Concrete tile lining			Brick tile lining			Brunt clay tile lining			
	With LDPE film			With LDPE film			With LDPE Film			
Types of data	100 m (2)	200 m (3)	Without film (4)	100 m (5)	200 m (6)	Without film (7)	100 m (8)	200 m (9)	Without film (10)	ce/cr (m) (11)
Ordinary soil	12.75	13.02	12.24	6.39	6.67	5.88	6.08	6.35	5.57	6.96
Hard soil	10	10.22	9.60	5.01	5.23	4.62	4.77	4.99	3.37	8.86
Impure lime nodules	8.9	9.10	8.55	4.47	4.66	4.11	4.25	4.44	3.89	9.96
Dry shoal with shingle	6.56	6.71	6.30	3.29	3.43	3.03	3.13	3.27	2.86	13.50
Slush and lahel	6.40	6.54	6.14	3.21	3.53	2.95	3.05	3.19	2.79	13.86

LPDE = Low density polyethylene.

Table 3 | Modeling parameters of the trapezoidal channel

Flow factors				Average roughness of height	Cost of terms			
Q (m^3/s)	S_0	g (m/s^2)	ϑ (m^2/s)	ε (mm)	$\frac{C_{wE}}{C_e}$	$\frac{C_l}{C_e}$	$\frac{C_e}{C_r}$	$\frac{C_{ws}}{C_e}$
100	0.001	9.79	1.1×10^{-6}	1	2	12	7	10

Note: For water at 20 °C.

channel area (A_*) presents a direct linear relation with T_{w*}: the higher the T_{w*}, the greater the A_* value. In the case of C_* variations, however, there is no direct linear relationship, where C_* tends to yield a constant value for T_{w*} values of approximately 0.45. Compared with no additional constraint model (Model I) in Table 5, it is clear that decreasing the channel top width would decrease the total cost by 30%.

In order to safely convey the required discharge through the channel, it is necessary to make sure that the actual average velocity in the channel will not exceed the maximum permissible velocity. To analyze this effect, Model III was evaluated (in which different values of velocity are introduced as additional constraints) and the results are presented in Table 6 and Figure 5. According to this model, decreasing flow velocity leads to higher construction cost values. Again, comparing the results of Tables 4–6, it is seen that for higher velocity values, the influence of introducing velocity as an additional constraint diminishes due to the higher cost needed for constructing a specific channel for delivering high-velocity flows. Nevertheless, for velocity values smaller than 2.1 m/s, the cost increases up to 30%,

Table 4 | Optimum results for trapezoidal channels design (Method I and II) with no additional restriction (Model I)

Parameters	Method I (Swamee *et al.* (2000), Model I)	Method II (GA, Model I)
b (m)	5.829	5.159
y (m)	3.878	3.784
m	0.512	0.540
A (m^2)	30.304	27.253
Fr	0.6	0.68
V (m/s)	3.3	3.66
Cost	429.27	417.26

Note: Cost equivalent $k = C_*\times\lambda^2$; $C = C_e$.k.

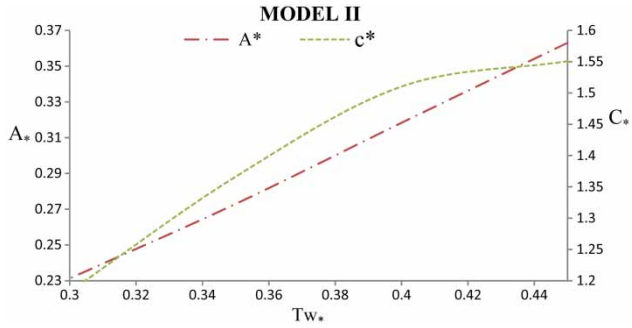

Figure 4 | Effect of top width in optimal solution.

Table 5 | Optimization result for different values of top width as additional restriction (Model II)

	When top width is:			
Parameters	$T_{W*} \le 0.45$	$T_{W*} \le 0.4$	$T_{W*} \le 0.35$	$T_{W*} \le 0.3$
b (m)	4.388	3.752	3.100	2.575
y (m)	4.086	4.324	4.070	3.625
m	0.337	0.300	0.300	0.300
A (m^2)	23.655	21.895	17.718	13.374
V (m/s)	4.222	4.58	5.636	7.466
Cost	391.855	381.743	345.338	298.821

Note: Cost equivalent $C = C_e\times$k; $k = C_*\times\lambda^2$.

Table 6 | Optimization result for different values of velocity as additional restriction (Model III)

	When velocity is:				
Parameters	$V \le 3.5$	$V \le 3$	$V \le 2.9$	$V \le 2.5$	$V \le 2.1$
b (m)	5.399	5.135	3.434	8.792	10.478
y (m)	3.699	3.084	3.545	3.434	3.657
m	0.632	1.804	1.766	0.823	0.690
A (m^2)	28.625	33.291	34.439	39.949	47.559
Fr	0.66	0.67	0.63	0.48	0.38
Cost	429.194	505.620	511.181	537.979	570.086

Note: Cost equivalent $C = C_e.k$; $k = C_*\times\lambda^2$.

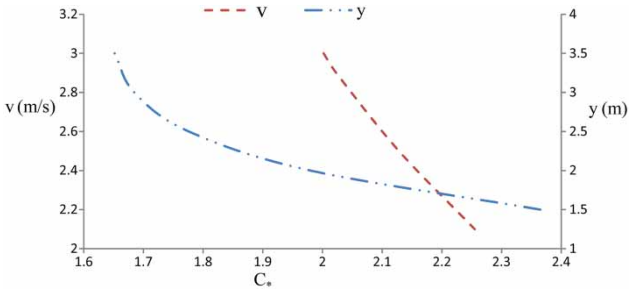

Figure 5 | Model (III, V) performances for various depth and velocity.

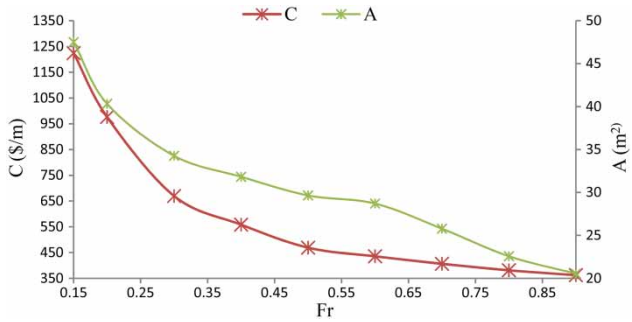

Figure 6 | Changes in the total cost of construction and the area channel with different Froude numbers.

because it requires greater cost and effort to deliver low-velocity (and high-normal depth, consequently) flows through the channel. Figure 5 illustrates that increasing flow velocity has a direct effect on C_*, while there is an inverse relation between the depth variations vs. C_*.

Table 7 sums up the optimization results of channel design for different Froude number (Fr) values. As a predecessor, it is clear that for better stability of the designed channel, the flow regime must be sub-critical, for which Fr should be less than unity ($Fr < 1$). From Figure 6, it can be seen that total area and the cost of channel construction increase with the reduction of the maximum Fr number value, due to the reduction in velocity of the channel and subsequent increase in the cross-sectional area. It is clear from the table that the cost reduction with increasing the smaller Fr number is more significant than those observed for larger Fr values increasing. The total cost of construction obtained by Model IV for $Fr \leq =0.15$ is approximately 1.93 times more than that obtained from Model I (Fr = 0.68). In Table 7, it is clear that for $Fr \leq =0.3$ side slopes (m) tend to zero ($m \to 0$), for which the trapezoidal cross section would transform to a rectangular cross section. Comparison between Model IV for $Fr = 0.9$ (Table 6) and Model I with $Fr = 0.68$ (no additional restriction) shows that total cost of construction decreases by approximately 21%.

Figure 7 plots the variation of b_* versus y_{n*}, with different Froude numbers around the critical flow regime ($m =$ 0.5). Results indicate that for near critical state condition, as b_* increases y_{n*} decreases.

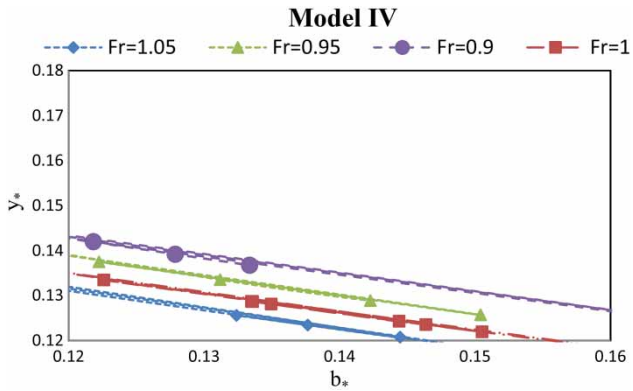

Figure 7 | Change in depth with width of the channel for side slope $m = 0.5$.

Table 7 | Optimization result for different Froude numbers for subcritical–supercritical flow condition as additional restriction (Model IV)

	When *Fr* is:								
Parameter	***Fr*** **≤ 0.15**	***Fr*** **≤ 0.2**	***Fr*** **≤ 0.3**	***Fr*** **≤ 0.4**	***Fr*** **≤ 0.5**	***Fr*** **≤ 0.6**	***Fr*** **≤ 0.7**	***Fr*** **≤ 0.8**	***Fr*** **≤ 0.9**
b (m)	2.368	2.573	3.554	3.175	4.532	4.554	4.404	4.927	4.675
y (m)	20.070	15.678	9.648	7.743	5.430	4.496	4.078	3.717	3.553
m	1.9×10^{-5}	4.44×10^{-5}	9.09×10^{-5}	0.121	0.172	0.408	0.471	0.309	0.313
V (m/s)	2.102	2.477	2.914	3.138	3.368	3.479	3.873	4.425	4.860
A (m^2)	47.503	40.314	34.263	31.823	29.650	28.707	25.784	22.568	20.546
P (m)	42.48	33.909	22.837	18.765	15.543	14.260	13.416	12.702	12.115
Cost	1224.326	976.2052	669.768	558.526	469.243	435.686	406.570	381.325	362.526

Note: Cost equivalent $C = C_e.k$; $k = C_* \times \lambda^2$.

Table 8 | Optimization result for different values of depths as additional restriction (Model V)

	When depth is:				
Parameter	$y \leq 1.5$	$y \leq 2$	$y \leq 2.5$	$y \leq 3$	$y \leq 3.5$
b (m)	18.60	13.22	9.77	7.55	5.91
y (m)	1.49	1.98	2.49	2.98	3.49
m	0.55	0.54	0.53	0.5	0.53
A (m^2)	29.05	28.41	27.72	25.27	27.25
Cost of evaporation (C_{we})	40.29	30.55	24.72	21.35	19.21
Cost	597.87	417.59	449.01	425.91	417.59

Note: Cost equivalent $k = C_* \times \lambda^2$; $C = C_e.k$, $C_{we} = C_{we*} \times \lambda^2$.

Table 9 | Optimization result without cost of seepage

Parameter	**Model VI**
b (m)	4.770
y (m)	4.070
m	0.505
A (m^2)	27.779
Cost	218.68

Table 8 sums up the optimization results for Model V, where y_{max} is considered a constraint in the event that unfavorable strata depth of channel should not go beyond a certain limit, because the excavation may not be economical or due to some other problem, such as the presence of shallow ground water table. This may require restriction on the maximum permissible flow depth. Therefore, the bottom width of the channel should be significantly increased to provide the necessary cross-sectional area for conveying the required flow discharge, which leads to increasing section area as well as the total cost and evaporation loss.

According to Table 9, Model VI, which eliminates seepage from the objective function, caused a decrease in total cost (47% in the problem presented in this paper). It clearly shows the significant effect of seepage on the optimal parameter of a channel.

The best state and minimum cost of each model are listed in Table 10. It can be observed that Models I, III, and V produce bottom widths of 5.159, 5.399 and 5.917 m, while Models II, IV, and VI produce 2.575, 4.927, and 4.77 m, respectively. The depths of flow are the same, but the side slopes given by Models II and IV have smaller magnitudes, in comparison with the other models. The total cross-sectional area obtained by Models II and IV (13.374 m^2 and 22.568 m^2, respectively) are approximately 50% and 17%, less than I and V models.

APPLICATIONS

In this section, several examples with different discharge values and longitudinal bed slopes (Models VII and VIII), which are considered as a constant problem in the previous models, are analyzed and the optimal dimensions calculated based on the new discharges and the longitudinal bed slopes. As can be observed from Figure 8, increasing of discharge values leads to growth trend in optimal cost, cross section area, and the top width of channel; while a decreasing trend is observed in the Froude number. For example, for a discharge of 300 (m^3/s) compared to the discharge of 80 (m^3/s), the cost has been increased by approximately 79%. The depth and width of the channel for the discharge of 200 (m^3/s) are equal to 6.92 m and 4.98 m and for the

Table 10 | Optimized parameters for various models – Method II for model

Parameters	**I (No restriction)**	**II ($T_* \leq 0.45$)**	**III ($V \leq 3.5$)**	**IV ($Fr \leq 0.8$)**	**V ($y \leq 3.5$)**	**VI**
b (m)	5.159	2.575	5.399	4.927	5.917	4.770
y (m)	3.784	3.625	3.699	3.717	3.497	4.070
m	0.540	0.300	0.632	0.309	0.535	0.505
A (m^2)	27.253	13.374	28.625	22.568	27.250	27.779
P (m)	9.459	7.154	9.77	12.702	13.853	13.889
T (m)	4.086	4.77	4.675	7.22	9.66	8.84
V (m/s)	3.66	7.466	3.5	4.425	3.665	3.579
Cost	417.26	298.821	429.194	381.325	417.594	218.68

Note: Cost equivalent $C = C_e \times k$; $k = C_* \times \lambda^2$.

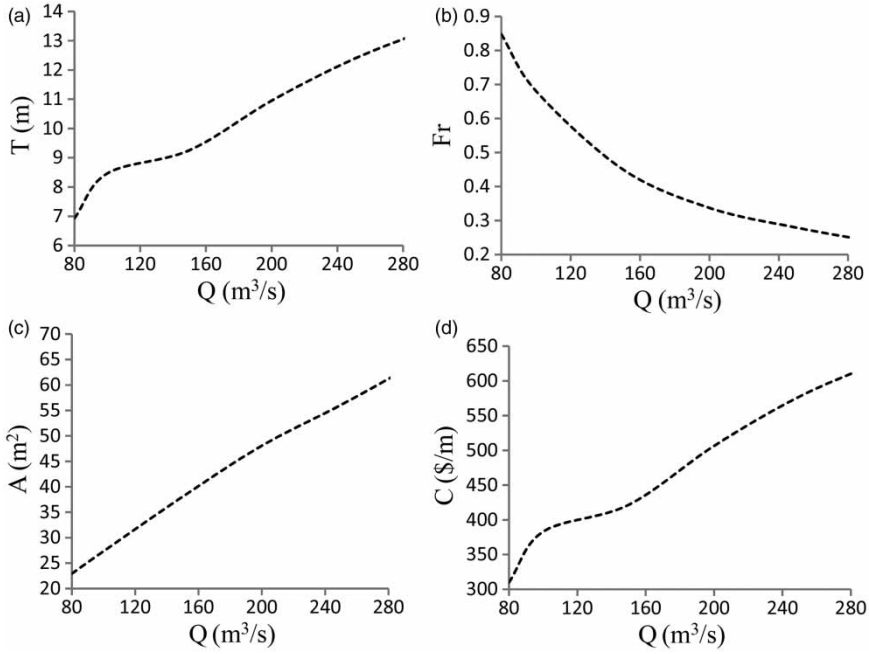

Figure 8 | Changes in the top width (a), the Froude number (b), the cross section area (c) and the total cost of construction (d) with different discharges ($S_0 = 0.001$).

discharge of 100 (m^3/s) are equal to 5.159 m and 3.784 m, which represents an increment in channel dimensions. However, the amounts of side slopes are close to each other and equal to about 0.5. For $Q = 250$ (m^3/s), the Froude number is 0.27, which has been decreased by 60% compared to the discharge of 100 (m^3/s). In the next model, different longitudinal bed slopes ranging from 0 to 0.0016 are examined for discharges of 100 m^3/s and 250 (m^3/s) and the optimum size obtained. It is also seen that there is a reduction in optimal cross section area and cost of channel construction and an increased Froude number and velocity by increasing longitudinal bed slope (Tables 11 and 12). For example, for $S_0 = 0.0013$, depth, bottom width, and slope are 4.89 m, 3.60 m and 0.53, respectively. For the discharge of 100 (m^3/s) and $S_0 = 0.0016$ compared to $S_0 = 0.0001$, it can be seen that there is a significant decline in the cost by 45%. Comparison between the discharge of 100 (m^3/s) with bed slope of 0.001 (Table 2) and discharge of 250 (m^3/s) with bed slope of 0.0016 shows that the cost and area cross section are raised, respectively, by approximately 36% and 41%, however the Froude number has been decreased by 48%. Here, the final results are shown

Table 11 | Optimization result for different values of side slope as ($Q = 100$ m^3/s), Model VII

S_0	Cost ($/m)	m	Fr	V (m/s)	A (m^2)	b (m)	y (m)	T (m)
0.0001	702.90	0.55	0.22	1.48	67.55	8.27	5.86	14.77
0.0003	551.94	0.54	0.37	2.25	44.33	6.49	4.85	11.78
0.0005	492.10	0.53	0.47	2.76	36.13	5.92	4.36	10.63
0.0007	456.81	0.53	0.56	3.16	31.58	5.55	4.07	9.93
0.0009	432.16	0.53	0.64	3.50	28.57	5.29	3.87	9.45
0.0011	413.45	0.53	0.71	3.79	26.35	5.06	3.72	9.08
0.0013	398.67	0.53	0.77	4.05	24.65	4.89	3.60	8.78
0.0014	392.15	0.53	0.80	4.17	23.93	4.82	3.55	8.65
0.0016	381.06	0.54	0.85	4.40	22.69	4.69	3.45	8.43

Table 12 | Optimization result for different values of side slope ($Q = 250\ m^3/s$), Model VII

S_0	Cost ($/m)	m	Fr	V (m/s)	A (m^2)	b (m)	y (m)	T (m)
0.0001	1082.93	0.58	0.09	1.81	137.86	11.84	8.25	21.55
0.0003	832.71	0.60	0.15	2.78	89.71	8.71	6.95	17.08
0.0005	738.90	0.56	0.19	3.39	73.57	8.55	6.11	15.49
0.0007	683.05	0.56	0.23	3.89	64.25	8.06	5.70	14.45
0.0009	645.14	0.56	0.26	4.28	58.31	7.52	5.49	13.70
0.0011	618.72	0.53	0.29	4.62	54.05	7.52	5.24	13.09
0.0013	594.69	0.56	0.31	4.94	50.57	6.91	5.15	12.70
0.0014	585.17	0.54	0.32	5.08	49.14	6.99	5.03	12.52
0.0016	567.83	0.55	0.35	5.36	46.61	6.65	4.94	12.18

Table 13 | The final results for optimization design of trapezoidal cross section

The variation of cost for proposed models ($Q = 100$ m, $S_o = 0.001$)

Optimization models	Increases range	Cost decrease	Cost increase
Top width (m) Model II	(4.78–7.17)		*
V (m/s) Model III	(2.1–3.5)	*	
Froude number Model IV	(0.15–1)	*	
Depth (m) Model V	(1.5–3.5)	*	

in Table 13. It can be concluded from Table 13 that cost change for other values of discharge with bed slopes might be the same as the models (II to V) with discharge of 100 m^3/s and $S_O = 0.001$.

CONCLUSIONS

In the present research, the effect of parameter restrictions on optimal design of trapezoidal channels was investigated. The proposed non-linear optimization formulation consists of minimizing the cost of lining, the depth-dependent unit volume earthwork, water lost by seepage, and evaporative losses of the open channel that are constrained by uniform flow conditions and the resistance equation. For the aforementioned optimization issue, six different models were proposed. These non-linear models were evaluated as including no restriction, constrained normal depth, constrained velocity of flow, constrained Froude number, and constrained top width. The optimization formulations corresponding to all of the models are investigated in the present research and solved using GA. The results indicate that for Models III and V (with constrained velocity and normal depth), the total cost of construction is high and for Models II and IV (with constrained top width and Froude number ($Fr > 0.7$)), the cost of construction in the open channels is smaller. Also, the results indicate that a model which disregards seepage in the objective function causes a considerable decrease in the cost. The obtained result suggests that seepage cost plays an important role on optimal design of open channels. Also, the different applications in the last two models for different discharge with constant bed slope ($S_O = 0.001$) and varying longitudinal bed slopes with constant discharge ($Q = 100\ m^3/s$, $Q = 250\ m^3/s$) was evaluated. It was concluded that with increasing discharge and bed slope, cost of channel construction increases and decreases, respectively.

It is to be noted that the present study is conducted for a specified set of input values and it can be easily extended to any other combination of input design parameters. Also the proposed models for design of open channels are simpler to implement and effective for practical applications, thus it can be used for reliable design of irrigation channels.

REFERENCES

Aksoy, B. & Altan-Sakarya, A. B. 2006 Optimal lined channel design. *Canadian Journal of Civil Engineering* **33**, 535–554.

Azamathulla, H. Md. 2012 Gene expression programming for prediction of scour depth downstream of sills. *Journal of Hydrology* **460–461C**, 169–172.

Azamathulla, H. Md. 2013 Gene-expression programming to predict friction factor of Southern Italian Rivers. *Neural Computing & Applications* **23** (5), 1421–1426.

Azamathulla, H. Md. & Ahmad, Z. 2013 Estimation of critical velocity for slurry transport through pipeline using adaptive neuro-fuzzy interference system and gene-expression programming. *Journal of Pipeline Systems Engineering and Practice* **4** (2), 131–137.

Bhattacharjya, R. K. & Satish, M. G. 2007 Optimal design of a stable trapezoidal channel section using hybrid optimization techniques. *Journal of Irrigation and Drainage Engineering* **133** (4), 323–329.

Chow, V. T. 1973 *Open Channel Hydraulics.* McGraw-Hill, New York, USA.

Christensen, B. A. 1984 Discussion of flow velocities in pipelines by Richard D. Pomeroy. *Journal of Hydraulic Engineering* **110** (10), 1510–1512.

Dimitriadis, P., Tegos, A., Oikonomou, A., Pagana, V., Koukouvinos, A., Mamassis, N., Koutsoyiannis, D. & Efstratiadis, A. 2016 Comparative evaluation of 1D and quasi-2D hydraulic models based on benchmark and real-world applications for uncertainty assessment in flood mapping. *Journal of Hydrology* **534**, 478–492. doi:10.1016/j.jhydrol.2016.01.020, 2016.

Froehlich, D. C. 1994 Width and depth-constrained best trapezoidal section. *Journal of Irrigation and Drainage Engineering* **120** (4), 828–835.

Fulford, J. M. & Sturm, T. W. 1984 Evaporation from flowing channels. *Journal of Energy Engineering* **110** (1), 1–9.

Garg, S. P. & Chawla, A. S. 1970 Seepage from trapezoidal channels. *Journal of Hydraulic Engineering* **96** (6), 1261–1282.

Goldberg, D. E. 1989 *Genetic Algorithms in Search, Optimization, and in Machine Learning,* 1st edn. Addison Wiley Longman, Boston, MA, USA.

Holland, J. H. 1975 *Adaptation in Natural and Artificial Systems.* University of Michigan Press, Ann Arbor, MI, USA.

Ikebuchi, S., Seki, M. & Ohtoh, A. 1988 Evaporation from Lake Biwa. *Journal of Hydrology* **102** (1), 427–449.

Jain, A., Bhattacharjya, R. K. & Sanaga, S. 2004 Optimal design of composite channels using genetic algorithm. *Journal of Irrigation and Drainage Engineering* **130** (4), 286–295.

Janga Reddy, M. & Nagesh Kumar, D. 2009 Performance evaluation of elitist-mutated multi objective particle swarm optimization for integrated water resources management. *Journal of Hydroinformatics* **11** (1), 78–88.

Kacimov, A. R. 1992 Seepage optimization for trapezoidal channel. *Journal of Irrigation and Drainage Engineering* **118** (4), 520–526.

Kaveh, A. & Talatahari, S. 2010 A novel heuristic optimization method: charged system search. *Acta Mechanica* **213** (3–4), 267–289.

Kennedy, J. & Eberhart, R. C. 1995 Particle swarm optimization. In: *Proceedings of IEEE International Conference on Neural Networks, Piscataway, NJ, USA*, pp. 1942–1948.

Koza, J. R. 1992 *Genetic Programming on the Programming of Computers by Means of Natural Selection.* The MIT Press, Cambridge, MA, USA, 840 pp.

Monadjemi, P. 1994 General formulation of best hydraulic channel section. *Journal of Irrigation and Drainage Engineering* **120** (1), 27–35.

Morel-Seytoux, H. J. 1964 Domain variations in channel seepage flow. *Journal of Hydraulic Engineering* **90** (2), 55–79.

Nixon, J. B., Dandy, G. C. & Simpson, A. R. 2000 A genetic algorithm for optimizing off-farm irrigation scheduling. *Journal of Hydroinformatics* **3**, 11–22.

Nourani, V., Talatahari, S., Monadjemi, P. & Shahradfar, S. 2009 Application of ant colony optimization to optimal design of open channels. *Journal of Hydraulic Research* **47** (5), 656–665.

Roushangar, K. & Koosheh, A. 2015 Evaluation of GA-SVR method for modeling bed load transport in gravel-bed rivers. *Journal of Hydrology* **527**, 1142–1152.

Schedule of rates 1997 *Irrigation Department.* Government of Uttar Pradesh, Lucknow, India.

Sharifi, S. B., Sterling, M. & Knight, D. W. 2011 Prediction of end-depth ratio in open channels using genetic programming. *Journal of Hydroinformatics* **13** (1), 36–48.

Sharma, H. D. & Chawla, A. S. 1979 Canal seepage with boundary of finite depth. *Journal of Hydraulic Engineering* **105** (7), 877–897.

Subramanya, K., Madhav, M. R. & Mishra, G. C. 1973 Studies on seepage from canals with partial lining. *Journal of Hydraulic Engineering* **99** (12), 2333–2351.

Swamee, P. K. 1994 Normal-depth equations for irrigation canals. *Journal of Irrigation and Drainage Engineering* **120** (5), 942–948.

Swamee, P. K., Mishra, G. C. & Chahar, B. R. 2000 Comprehensive design of minimum cost irrigation canal sections. *Journal of Irrigation and Drainage Engineering* **126** (5), 322–327.

Wachyan, E. & Rushton, K. R. 1987 Water losses from irrigation canals. *Journal of Hydrology* **92** (3–4), 275–288.

Warnaka, K. & Pochop, L. 1988 Analysis of equations for free water evaporation estimates. *Water Resources Research* **24** (7), 979–984.

Wu, Z. Y. & Simpson, A. R. 2002 A self-adaptive boundary search genetic algorithm and its application to water distribution systems. *Journal of Hydraulic Research* **40** (2), 191–203.

First received 3 July 2016; accepted in revised form 7 December 2016. Available online 6 March 2017